Journal of Catalysis **201,** 113–127 (2001)
doi:10.1006/jcat.2001.3238, available online at http://www.idealibrary.com on IDEAL®

Structural Properties and Catalytic Behaviour of Iridium Black in the Selective Reduction of NO by Hydrocarbons

C. Wögerbauer,* M. Maciejewski,* A. Baiker,*,[1] and U. Göbel†

*Laboratory of Technical Chemistry, Swiss Federal Institute of Technology, ETH-Zentrum, CH-8092 Zürich, Switzerland; and †dmc^2 Degussa Metals Catalyst Cerdec AG, Rodenbacher Chaussee 4, D-63457 Hanau-Wolfgang, Germany

Received January 25, 2001; revised March 20, 2001; accepted March 26, 2001; published online May 31, 2001

Several mechanical mixtures of Ir black or IrO_2 with various mixing materials like silica xerogel, alumina, and H-ZSM-5 were tested for their activity in the selective reduction of NO by propene. Independent of the mixing material used the unsupported Ir showed outstanding DeNOx activity compared to their supported counterparts. The conversion of NO to N_2 under lean conditions as well as oxidizability and reducibility of the Ir–IrO_2 system was found to depend strongly on the Ir crystallite size. With increasing crystallite size, selectivity to N_2 is greatly enhanced mainly by the suppression of a reaction pathway leading to the production of NO_2. Tailoring of Ir crystallite size by controlled sintering of Ir black afforded highly active Ir catalysts without the need for further conditioning on stream. Among unsupported platinum group metals iridium showed the best performance in NO_x removal. The catalytic behaviour of Ir black was compared to the behaviour of Pt black, Pd black, and Rh black. Unsupported IrO_2 with relatively large crystallite size (24 nm) was inactive for the selective reduction of NO with propene. Only IrO_2 with small crystallite size (below ca. 11 nm) and high surface area could be activated by on-stream conditioning. Ir black and IrO_2 were characterized by XRD, TEM, SEM, thermal analysis, and krypton adsorption measurements. It was shown that it is unlikely that NO_2 is an intermediate in the reduction of NO.

Key Words: **unsupported iridium; iridium black; IrO_2; platinum group metals; platinum black; rhodium black; palladium black; reduction of NO; HC-SCR; lean DeNOx; NO_x reduction.**

1. INTRODUCTION

Despite the great success which has been achieved in automotive pollution control over the last 30 years, especially due to the excellent performance of the three-way catalyst for Otto engines, there is still an urgent need to improve catalytic aftertreatment systems for exhaust gases. This is especially due to ever more stringent emission requirements of future legislation (1). In addition to the removal of the emission of harmful by-products of combustion (mainly unburnt hydrocarbons, NO_x, CO, and particulate emissions) there is a demand for a reduction in fuel consumption and CO_2 emission levels (1). Lean burn engines, i.e., diesel and gasoline direct injection engines, seem to constitute a key factor for achieving these goals. They offer a significant advantage in fuel consumption compared to gasoline engines operated at a stochiometric factor of $\lambda = 1$. Unburnt hydrocarbons can be removed by standard oxidation catalysts but the cardinal problem with direct injection engines concerning pollution control is the further reduction of raw NO_x emissions under lean conditions to levels complying with legislation (1). Besides other measures for the reduction of NO_x emissions, selective catalytic reduction of NO_x using hydrocarbons as reducing agents is a promising option for achieving emission values complying with stringent NO_x limits. Platinum group metals (PGM) still continue to attract attention as active catalysts in this reaction. Precious metal catalysts are the only catalysts known which can tolerate the versatile operation conditions of direct injection engines and hence the variable exhaust gas composition. Under full load, gasoline direct injection engines are operated at $\lambda \leq 1$ to ensure full power supply. Therefore, it is necessary that in addition to the activity under lean conditions the prospective catalyst offers full three-way functionality under stoichiometric air to fuel conditions. This is the case for PGMs. Among the family of PGMs Pt has been studied most exhaustively but comparably little attention has been paid to Ir, although Ir catalysts have been already used commercially in Japan and Europe, and the first accounts of the usefulness of Ir catalysts in the reduction of NO date back to 1976 when Tauster and Murrell (2) reported on the selectivity of Ir–Al_2O_3 in the reduction of NO with CO under lean conditions. This was later confirmed by Lester *et al.* (3) for a more complex synthetic exhaust gas and by Taylor and Schlatter (4). However, only until very recently no systematic work on Ir catalysts has been published. This is possibly due to the scarcity of this element and the fact that in screening studies usually supported Ir catalysts after prereduction or oxidation were found to be almost inactive (5–7). Spurred by

[1] To whom correspondence should be addressed: Fax: +41 1 632 11 63. E-mail: baiker@tech.chem.ethz.ch.

0021-9517/01 $35.00

the commercial application and unexpected good laboratory results, the interest in Ir has been increasing steadily over the last years. Takami *et al.* (8) developed a Pt/Ir/Rh on MFI-zeolite catalyst which met the Japanese emission standards and Hori *et al.* presented a new Ir-based catalyst for gasoline lean burn engines (9). Ir catalysts were found to be stable in SO_2 and H_2O-containing atmosphere (10). Catalyst activation was achieved by high temperature pretreatments as reported by Nakatsuji (11) or by *in situ* activation of Ir during catalytic tests (12). The *in situ* activation is very sensitive to the feed gas composition (13) and usually both, *in situ* activation and high temperature pretreatment, lead to crystallite growth and the development of a certain $Ir : IrO_2$ ratio.

Here we demonstrate that unsupported Ir black yields high NO_x reduction activity and that the support is of minor influence, as long as it is not inherently detrimental to the NO reduction process, for instance, by unselective consumption of the reductant. To stress the uniqueness of the high activity of unsupported Ir we compare the results for Ir to other unsupported PGMs which are, in their supported form, well known for their good performance in the selective reduction of NO (Pt black, Pd black, Rh black). Furthermore, we show the dependence of selective NO reduction on Ir crystallite size by correlation of DeNOx activity, metallic surface area, and crystallite size of various well-defined samples of Ir black. Finally, some aspects of the role of the NO_x component, i.e., NO, N_2O, and NO_2, in the reduction process are discussed.

2. EXPERIMENTAL

2.1. Catalyst Preparation

Supported Ir catalysts used in this study were prepared by wet impregnation of H-ZSM-5 ($Si/Al = 34$, 400 m^2/g, Chemie Uetikon). An aqueous solutions of $IrCl_3 \cdot 3H_2O$ was used for the impregnation of the zeolite. The iridium chloride used was obtain from Alfa Aesar. After impregnation of the zeolite, the catalysts were dried in air at 120°C for 12 h; they were then calcined in air at 500°C for 2 h. The metal loading was determined by ICP-AAS to be 4.6 wt%.

Ir black and IrO_2 were supplied by Alfa Aesar. These materials were either used as received or, to produce a certain crystallite size, presintered by heating in He to the corresponding set temperature with a heating rate of 10 K/min and then quenched to room temperature. Samples of Ir black were prereduced at 300°C with 6% H_2 prior to the catalytic tests. Two batches of IrO_2 were used. They are denoted as IrO_2-A and IrO_2-B. IrO_2-A was found to be contaminated with Na (2.4 wt% on the basis of Na_2O). Although some influence of this impurity on the catalytic behaviour could not be ruled out, it was found that after conditioning, contaminated and uncontaminated samples showed similar catalytic behaviour, provided the morphology was the same. The conclusions drawn from the results presented here were thus not influenced by the Na impurities. This also emerged from a systematic study of the effect of Na promotion of Ir black, reported elsewhere (14). All other materials did not contain significant impurities.

To distinguish supported catalysts from mechanical mixtures, for supported catalysts a dash was used to separate metal and support (Ir-H-ZSM-5) and for mixtures a slash (Ir/H-ZSM-5).

2.2. Mixing Material

The silica gel, which was used as mixing material, was prepared by the sol-gel method. The gel was prepared as xerogel using a solution of tetramethylorthosilicate (22.83 g) in *i*-propanol (105 ml) as starting material. A solution of H_2O (13.01 g) and HNO_3 (1.45 g) in *i*-propanol (40 ml) was added under vigorous stirring for hydrolysis. After 6 h of hydrolysis trihexylamine (6.06 g in 40 ml *i*-propanol) was added and the gel was left to age for 6 days, dried in a vacuum oven at 50°C for another 5 days, and then calcined in air at 750°C for 3 h. The alumina (Degussa C) was supplied by Degussa-Hüls and H-ZSM-5 ($Si/Al = 34$) was supplied by Chemie Uetikon.

2.3. Catalytic Tests

For activity tests, 150 mg of the catalyst (particle fraction between 0.066 and 0.177 μm) was held between two quartz wool plugs in a quartz reactor (6 mm i.d.). The mechanical mixtures were prepared by dilution of Ir black or IrO_2 with the mixing material (SiO_2 unless stated otherwise). A reactor filling with a mixture of unsupported Ir black or IrO_2 contained 7.5 mg Ir black or the corresponding amount of IrO_2 mixed with alumina, silica, or H-ZSM-5 to achieve a space velocity of approximately 80,000 h^{-1}. Unless stated otherwise, the feed gas contained 1800 ppm propene, 450 ppm CO, 300 ppm NO, 10% H_2O, 10.7% CO_2, 8% O_2, and N_2 as balance gas at a flow rate of 3 Nl/g min. *In situ* conditioning was achieved by treating the catalysts for 4 h at 450°C with the above feed gas (heating in reaction atmosphere). On-line analysis was performed with a Bruker IFS 66 FTIR spectrometer; details of the apparatus are described in Ref. (15). The activity was tested in both steady-state and temperature-programmed experiments. During steady-state experiments the temperature was gradually increased in steps of 50°C starting at 160°C with a holding time at each step of 1 h. Temperature-programmed activity tests were carried out with a heating rate of 5 K/min from 150 to 480°C. After the experiments the catalysts were quenched in N_2 to room temperature.

The total consumption of NO is given as X_{NO} and NO conversion to N_2 (yield, Y_{N_2}) was calculated according to the equation (superscript 0 denotes inlet flows):

$$Y_{N_2} = \left[\left(F^0_{NO} - \left(F_{NO} + F_{NO_2} + 2 \cdot F_{N_2O}\right)\right)/F^0_{NO}\right] \cdot 100.$$

The selectivity was calculated according to the equation:

$$S_{N_2} = Y_{N_2}/X_{NO} \cdot 100.$$

Temperatures of 50% conversion are denoted as T_{50}.

2.4. Characterization

X-ray diffraction (XRD). X-ray analysis was carried out on a Siemens D 5000 powder X-ray diffractometer using the Cu$K\alpha$ radiation in step mode between 20 and 80° 2Θ, with a step size 0.01° and 4 sec/step. The Ir crystallite size was estimated using X-ray diffraction line broadening of the Ir (111) reflection and the Scherrer equation taking 0.9 as a shape factor value.

BET measurements (BET). Krypton BET measurements on a Micromeritics ASAP 2000 were applied to determine the surface area of IrO_2, Ir black with various crystallite sizes, Pt black, Rh black, and Pd black. Krypton was used because of the expected low surface areas of the metal samples. Before measurement the samples were degassed *in vacuo* at 80°C for several hours. The results of the high surface area samples were in good agreement with results from N_2 physisorption measurements.

Transmission electron microscopy (TEM). TEM measurements were performed on a Microscope CM30ST (Philips), operated at $V = 300$ kV, point resolution approximately 2 Å. Samples were deposited on a holey carbon grid supported on a copper grid.

Scanning electron microscopy (SEM). SEM measurements were performed on a Hitachi S-900, operated at $V = 15$ kV. Samples were prepared according to the TEM measurements.

Thermal analysis (TA). Thermoanalytical experiments were carried out both isothermally and non isothermally (heating rate 5 or 10 K/min), on a Netzsch STA 409 thermoanalyzer equipped with a gas injector (PulseTA box, Netzsch) which allows for the injection of a defined sample gas volume into the carrier gas stream (16). The amount of injected gases (hydrogen, oxygen) was 1.0 ml. Gases evolved during reaction and/or injected into the system were monitored on-line with a Balzers QMG 420 quadrupole mass spectrometer connected to the thermoanalyzer by a heated (ca. 200°C) capillary.

3. RESULTS

3.1. Catalytic Behaviour of Unsupported Iridium and IrO_2 Using Various Mixing Materials

Experiments using supported iridium catalysts suggested that strongly sintered Ir favours high activity in the reduction of NO using propene as reducing agent and that the support is of little importance to achieve good performance (11, 12). In fact the influence of the support can be inherently detrimental due to unselective reductant consumption and stabilization of a high Ir dispersion. In order to minimize metal-support interactions in the study of the intrinsic catalytic activity of Ir and for proper fixed bed reactor operation, mechanical mixtures of Ir or IrO_2 with silicagel, alumina, and H-ZSM-5 were applied. The main function of the mixing material was to ensure the same flow conditions during catalytic tests as those with supported catalysts to be able to compare the obtained results. Each mixing material was tested for activity but no significant activity for the reduction of NO could be detected under the applied conditions. The results presented below were obtained from steady-state activity measurements using IrO_2-A (crystallite size, 11 nm; specific surface area, 29 m^2/g) and Ir black (3 nm, 36 m^2/g) as received without presintering and a standard Ir-H-ZSM-5 catalyst after calcination in air (9 nm IrO_2 crystallite size).

Influence of the conditioning procedure on the catalytic activity of unsupported iridium and IrO_2. Supported Ir-H-ZSM-5 showed a pronounced increase in selective reduction of NO to N_2 after 4 h on stream at 450°C. This is referred to as conditioning as described in Ref. (12). Conditioning led to metal agglomeration, crystallite growth, and the establishment of a certain Ir : IrO_2 ratio. Figure 1 shows the behaviour of a mechanical mixture of IrO_2-A and H-ZSM-5 before and after conditioning (Figs. 1a and 1b, respectively) compared to the behaviour of IrO_2-H-ZSM-5, prepared by calcination of supported Ir-H-ZSM-5 in air at 500°C, directly after calcination (Fig. 1c) and after conditioning (Fig. 1d). The mechanical mixture and the supported catalyst show similar behaviour but the mechanical mixture is much more susceptible to the conditioning procedure and exhibits higher activity and selectivity in a broader temperature range compared to the supported catalyst. Both catalysts showed bad selectivity to N_2 with the only by-product formed being NO_2; no N_2O was formed. Ir-H-ZSM-5 showed after calcination in air a maximum for NO conversion to N_2 (Y_{N_2}) of 25% at ca. 400°C, whereas IrO_2-A/H-ZSM-5 reached maximum values of 37% Y_{N_2} at 415°C. After conditioning, for both catalysts selectivity improved and the mechanical mixture showed a maximum value for Y_{N_2} of 74% (365°C) and the supported IrO_2 improved to 45% (395°C). Neither in the case of IrO_2-A/H-ZSM-5 nor in the case of IrO_2-H-ZSM-5 N_2O formation was witnessed after conditioning. Both catalysts showed a conversion maximum for propene at temperatures between 160 and 310°C characteristic for propene adsorption and oligomerisation on H-ZSM-5.

Influence of the mixing material. Figure 2 shows the results for Y_{N_2} of several mixtures of Ir black and IrO_2-A (both as received) with different mixing materials. These results represent the activity of samples after conditioning. From Fig. 2 it can be seen that the mixing material influences

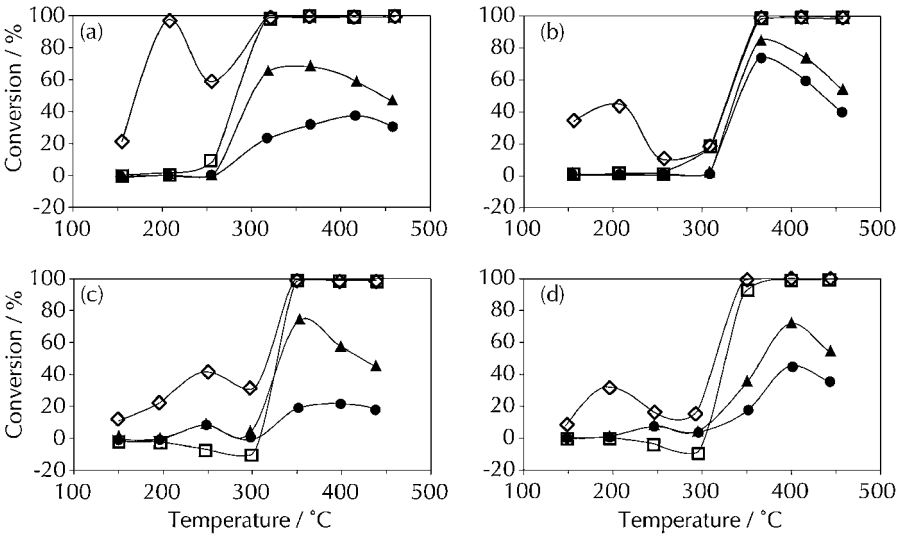

FIG. 1. Catalytic behaviour, i.e., the conversion of reductants and NO vs temperature, in steady-state measurements of IrO_2-A mixed with H-ZSM-5 as received (a) and after conditioning (b). Catalytic behaviour of Ir-H-ZSM-5 after calcination in air at 500°C (c) and after subsequent conditioning (d). The negative conversions for CO in (c) and (d) represent the production of small amounts of CO at 250 and 300°C. ●, Y_{N_2}; ▲, X_{NO}; ◇, $X_{Propene}$; □, X_{CO}.

Y_{N_2} but the influence of the Ir precursor (Ir black or IrO_2) prevails.

IrO_2 and Ir black as received were affected in different ways by the conditioning procedure. Both showed a pronounced increase in Y_{N_2} but IrO_2 gave high Y_{N_2} at ca. 350°C, whereas Ir black reached high Y_{N_2} at temperatures of 400°C and above. For the mixtures with IrO_2 it was found that after conditioning the material was partly reduced but to a lower extent as in the case of the calcined Ir-H-ZSM-5 (Table 1). The metallic Ir formed during conditioning could not be detected with XRD, indicating a very small crystallite size of the formed Ir phase. The amount of Ir formed during conditioning was determined by pulse thermal analysis. To achieve this the remaining amount of IrO_2 after reaction was determined by reduction of the catalyst at 250°C by pulses of H_2. IrO_2 crystallite size increased only slightly during conditioning. Ir black showed a pronounced increase in crystallite size and was partly oxidized. Although almost 30% of IrO_2 was formed during conditioning of Ir black mixtures with SiO_2 or Al_2O_3 (determined by pulse thermal analysis), its determination by XRD was impossible (SiO_2) or very difficult (Al_2O_3) due to the very small crystallite size of the produced IrO_2 phases.

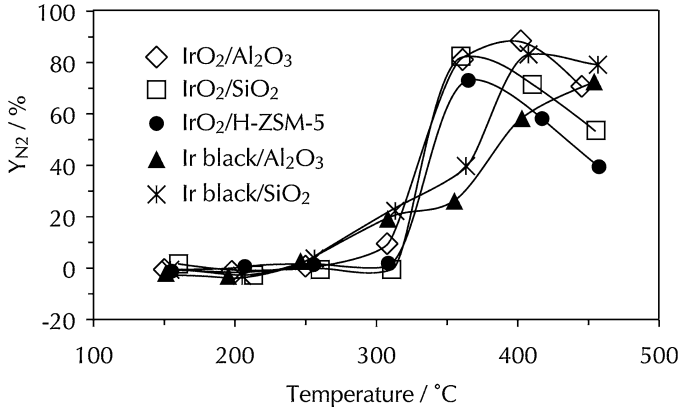

FIG. 2. NO conversion to N_2 (Y_{N_2} [%]) as a function of temperature in steady-state experiments of various mixtures of IrO_2-A as received and Ir black as received. The results represent the activity of the samples after conditioning.

3.2. Comparison of Catalytic Behaviour of Ir Black, Pt Black, Pd Black, and Rh Black

To compare the catalytic behaviour of unsupported Ir with other platinum metals, Pt black, Pd black, and Rh black were tested under the same experimental conditions as Ir

TABLE 1

Development of the Crystallite Size and the Ir : IrO_2 Ratio during Conditioning

Material	Crystallite size as received $Ir^a/IrO_2{}^b$	Crystallite size after conditioning $Ir^a/IrO_2{}^b$	Ir : IrO_2 after conditioning
IrO_2/SiO_2	11^b	am/13^b	20 : 80
IrO_2/Al_2O_3	11^b	am/15^b	25 : 75
IrO_2/H-ZSM-5	11^b	am/12^b	16 : 84
Ir black/SiO_2	3^a	11^a/am	73 : 27
Ir black/Al_2O_3	3^a	$12^a/6^b$	73 : 27
Ir-H-ZSM-5	9^a	$7^a/10^b$	30 : 70

Note. Crystallite size is given in [nm] and the Ir : IrO_2 is given as molar ratio [a] Ir and [b] IrO_2; am is the abbreviation for an XRD amorphous phase. The Ir : IrO_2 ratio was determined by reduction of the samples at 250°C by pulses of H_2.

TABLE 2

Formation of N_2 and By-Products of the Reduction of NO with Propene over Unsupported Platinum Group Metals after Prereduction (Reduced) and after Conditioning (Conditioned)

Platinum metal	NO_2 production	N_2O production	N_2 production	Y_{N_2}	T_{50} of CO	T_{50} of propene
Pt black	163 ppm	19 ppm	37 ppm	23%	200°C	240°C
reduced	172°C	272°C	272°C	272°C		
Pt black	163 ppm	21 ppm	41 ppm	26%	220°C	240°C
conditioned	320°C	273°C	273°C	273°C		
Pd black	0 ppm	21 ppm	17 ppm	11%	210°C	240°C
reduced		272°C	272°C	272°C		
Pd black	0 ppm	23 ppm	16 ppm	10%	240°C	240°C
conditioned		272°C	272°C	272°C		
Rh black	107 ppm	8 ppm	47 ppm	29%	210°C	285°C
reduced	365°C	316°C	316°C	316°C		
Rh black	133 ppm	traces	31 ppm	19%	285°C	335°C
conditioned	365°C	<5 ppm	365°C	365°C		
Ir black	175 ppm	12 ppm	103 ppm	63%	155°C	225°C
reduced	320°C	260°C	410°C	410°C		
Ir black	90 ppm	traces	134 ppm	83%	240°C	285°C
conditioned	363°C	<5 ppm	407°C	407°C		

Note. The maximum values of production of the respective products are given together with the corresponding temperature and the influence of the conditioning procedure on the T_{50} temperature of reductant consumption is illustrated.

black for their ability to reduce NO with propene as reducing agent. The mixing material used in these experiments was silica xerogel, the metals were used as received. The mechanical mixtures were prereduced before the catalytic tests at 300°C with 6% H_2.

Except for Ir, unsupported PGMs showed only moderate activity for the reduction of NO by propene under oxidizing conditions. Ir black after prereduction and after conditioning showed the highest values of Y_{N_2} compared to all other PGMs with more than twice as much NO reduced selectively to N_2 compared to the second most active PGM in both cases (Table 2). After prereduction the activity changed in the sequence Ir $\gg$ Rh > Pt > Pd with the temperature of maximum N_2 production falling from Ir (410°C) over Rh (316°C) to Pt and Pd (both 272°C). After conditioning the sequence of maximum NO reduction to N_2 was Ir $\gg$ Pt > Rh > Pd. Only at ca. 270°C Pt and Pd showed a higher degree of N_2 production than Ir (Fig. 3). Conditioning did not affect the temperature of maximum Y_{N_2} (except for rhodium) but had a distinct positive effect on Y_{N_2} for Ir, a slight on Pt, a negative for Rh, and left Y_{N_2} unchanged for Pd. For Ir and Rh conditioning led to the almost complete disappearance of N_2O formation (only traces below 5 ppm N_2O were found between 300 and 360°C) and to a pronounced increase of the T_{50} temperatures of CO and propene conversion. Except for Pd, which did not show any formation of NO_2, with all PGMs the main by-product was NO_2. Table 3 shows that conditioning led to a pronounced sintering for all PGMs and that all metals except Pt were partly oxidized under the applied experimental conditions. Pt and Ir showed the highest degree of sintering followed by Pd and Rh.

3.3. Dependence of Catalytic Activity of Unsupported Iridium on Crystallite Size

A series of mechanical mixtures using Ir with crystallite sizes ranging from 5 to 45 nm was investigated for the influence of crystallite size on NO conversion and selectivity (mixing material SiO_2). As described in the experimental part, Ir black was heated to the temperatures given in

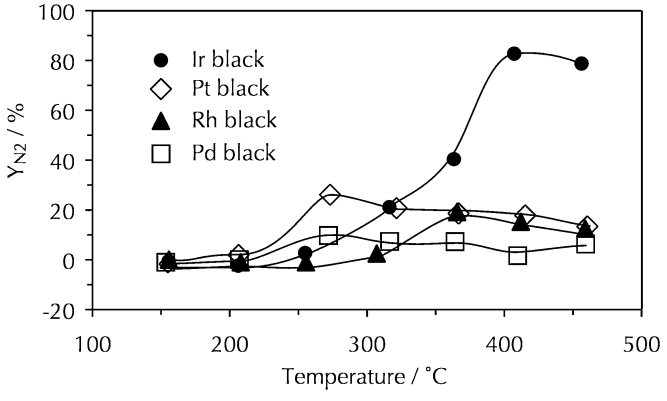

FIG. 3. NO conversion to N_2 (Y_{N_2} [%]) as a function of temperature in steady-state experiments of platinum group metals mixed with SiO_2 after conditioning.

TABLE 3

Specific Surface Areas of Platinum Group Metals and the Development of the Metal Crystallite Size and Metal to Oxide Ratio after Conditioning

PGM metal	Surface area [m^2/g]	Crystallite size/nm before and after conditioning [nm]		Metal: oxide after conditioning
Pt black	37.6 ± 0.2	7	26	100 : 0
Pd black	14.2 ± 0.1	13	33	51 : 49
Rh black	56.5 ± 0.3	6	12	42 : 58
Ir black	36.0 ± 0.3	3	11	73 : 27

Table 4 and than quenched to room temperature. Table 4 gives the resulting crystallite size and specific metal surface area. From the specific surface area, assuming spherical shape of the particles and equal proportions of the three low-index planes (111), (100), and (110) on the polycrystalline metal surface (17), metal dispersion (ratio of surface atoms to the total number of metal atoms) and approximate particle size were calculated. The effect of sintering on the morphology of Ir black can be seen from Fig. 4. The SEM measurements show a sponge-like network of connected particles which build up larger spheres. The dimensions of the particles depicted in the SEM measurements roughly reflect the calculated values of particle size if not the whole network, but the smaller interconnected bulb-like features are regarded as particles. With increasing degree of sintering the network becomes cruder and finally disintegrates. The TEM measurements of the sample with 5 nm crystallite size show a large amount of interfering fringes of the network of crystallites. The crystallite size estimated from the TEM micrographs is in good agreement with the size of 5 nm determined by XRD. The same holds true for the sample with 19 nm crystallite size. The sample with the largest crystallite size (45 nm) does not show any electron diffractions anymore due to the thickness of the sample.

Figure 5 represents the catalytic behaviour of four samples with different crystallite size after conditioning. The dependence of Y_{N_2} before conditioning is included as dashed line. For the reductants a slight shift of light off to lower temperatures can be seen with increasing crystallite size. The difference between the X_{NO} and the Y_{N_2} lines reflect the amount of by-products formed, mainly NO_2 and traces of N_2O (at ca. 260 and 310°C). With increasing crystallite size this difference diminishes, indicating an improvement in selectivity for the reduction of NO to N_2. For Y_{N_2} usually two regions can be distinguished. The first is the part below 310°C, where before conditioning Y_{N_2} is larger than after conditioning, and the second part above 310°C, where the situation is usually opposite. This phenomenon indicates that due to conditioning the catalyst loses its low temperature activity in exchange for an increased high temperature activity. With increasing crystallite size this effect becomes less pronounced and especially above 310°C, Y_{N_2} values before and after conditioning are very similar. In general, with increasing crystallite size, Y_{N_2} rises and with 45 nm it decreases again, which is most likely due to extensive loss of surface area (see Table 4). To better illustrate the dependence of activity on crystallite size, the amount of NO converted to N_2 per second was related to the surface area for each sample. The results shown in Fig. 6 indicate that with increasing crystallite size, i.e., with decreasing dispersion and decreasing surface area (Table 4), the amount of NO selectively reduced to N_2 increases distinctly. Figure 7 depicts the dependence of the catalytic activity on crystallite size at 360°C. The presented relationships illustrate that Y_{N_2} and X_{NO} reach a maximum in the crystallite size range of ca. 20 to 30 nm. Normalizing the amount of NO converted selectively to N_2 by surface area it becomes clear that at 360°C the catalysts with the highest degree of sintering exhibit the highest DeNOx activity. With increasing degree of sintering selectivity increases steadily.

Taking into account the total amounts of reaction products formed from NO over the whole experimental

TABLE 4

Temperature of Sintering, BET Surface Area [m^2/g], Calculated Particle Size [nm], Crystallite Size [nm], and Dispersion of Ir Black Samples with Different Crystallite Size

Iridium crystallite size after calcination [nm]	Temperature of sintering [°C]	BET surface area [m^2/g]	Calculated particle size [nm]	Dispersion [%]	Iridium crystallite size after conditioning [nm]
3	As received	36.0 ± 0.3	7	15.3	11
5	400	28.1 ± 0.3	9	12.2	12
13	520	11.6 ± 0.1	23	4.8	15
19	650	10.2 ± 0.1	28	3.9	19
27	750	6.8 ± 0.1	40	2.8	27
45	870	2.7 ± 0.1	99	1.1	45

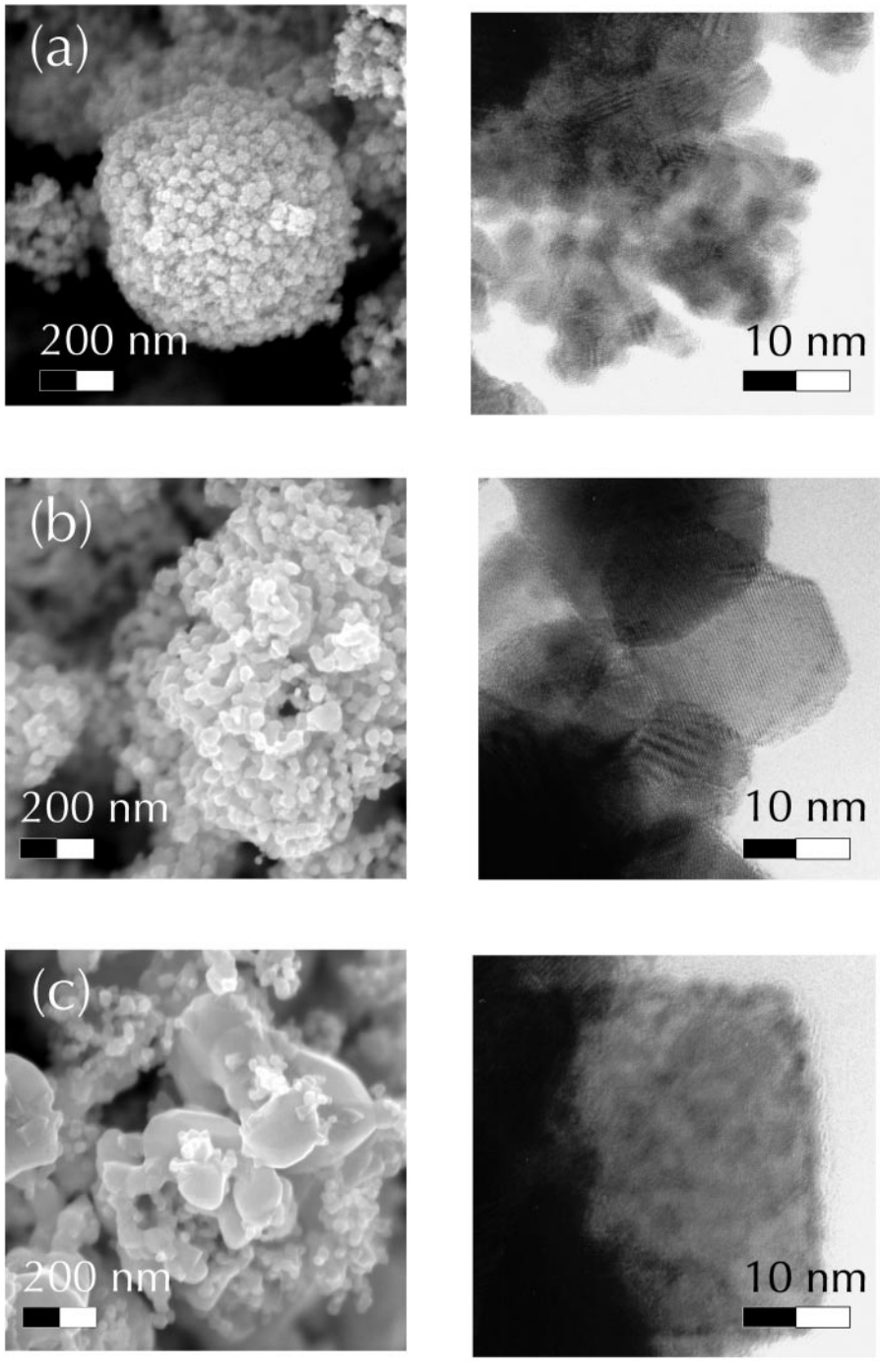

FIG. 4. Morphology of Ir black sintered to 5 nm (a), 19 nm (b), and 45 nm (c) Ir crystallite size as evidenced by SEM (left column) and TEM (right column). White and black scaling bars are 100 and 5 nm for SEM and TEM micrographs, respectively.

temperature range from 160 to 460°C during the period of an experiment it becomes clear that the major effect of conditioning of the Ir black samples consists in a pronounced increase in selectivity to N_2 formation. The selectivities calculated from the total amounts of N_2, N_2O, and NO_2 produced over Ir black with different crystallite sizes are presented in Fig. 8 for prereduced samples and samples after conditioning. The only sample with unchanged selectivity is the sample with the largest Ir crystallite size (45 nm). Before conditioning there is a steady increase in N_2 selectivity with increasing crystallite size up to 45 nm. After conditioning N_2 selectivity reached a maximum for 27 nm

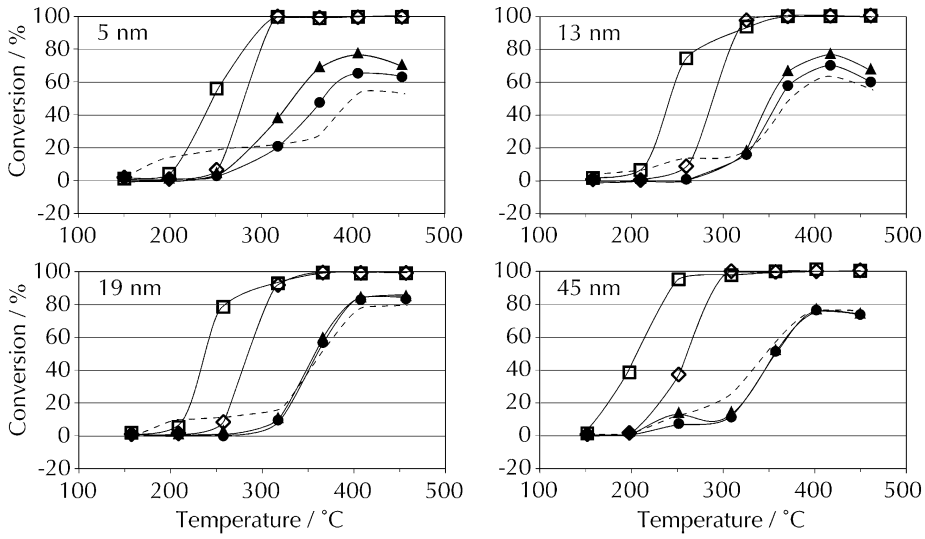

FIG. 5. Catalytic behaviour in steady-state experiments after conditioning of Ir black with different crystallite sizes mixed with SiO_2. The dashed line represents Y_{N_2} directly after prereduction of the sample to illustrate the changes in selective reduction of NO due to conditioning. ●, Y_{N_2}; ▲, X_{NO}; ◇, $X_{Propene}$; □, X_{CO}; --, Y_{N_2} prereduced.

and than declined for 45 nm crystallites due to the almost unchanged N_2O production of the sample (ca. 10 ppm at 250°C). In accordance with the increase in N_2 selectivity after conditioning, the selectivity for the production of NO_2 decreases and, except for the sample with 45 nm, the selectivity for N_2O decreases as well. Figure 9 illustrates the fact that after conditioning less NO is converted during an experiment. This loss in total NO conversion usually cannot be fully made up for by the improved selectivity therefore the total amount of N_2 produced is smaller after conditioning. Comparing the amount of NO reduced to N_2 over the full temperature range before and after conditioning leads, for instance, in the case of Ir black with 19 nm crystallite size, to the conclusion that ca. 20% less N_2 is produced after conditioning. Ir black with 45 nm crystallite size produces the same amount N_2 before and after conditioning.

3.4. Catalytic Activity of Unsupported IrO_2

The results of the catalytic activity (Y_{N_2} at 410°C) of three different samples of IrO_2 mixed with SiO_2 are summarized in Table 5. From the results presented it can be seen that at 410°C Y_{N_2} decreases sharply due to sintering of IrO_2-A as received. Using IrO_2-B with larger crystallite size and lower surface area yields even lower Y_{N_2}. Figure 10 shows that IrO_2-A as received is made up of extremely small crystallites and a few crystallites larger than 10 nm. This is in accordance with XRD measurements which showed that the material was very poorly crystalline and that at least

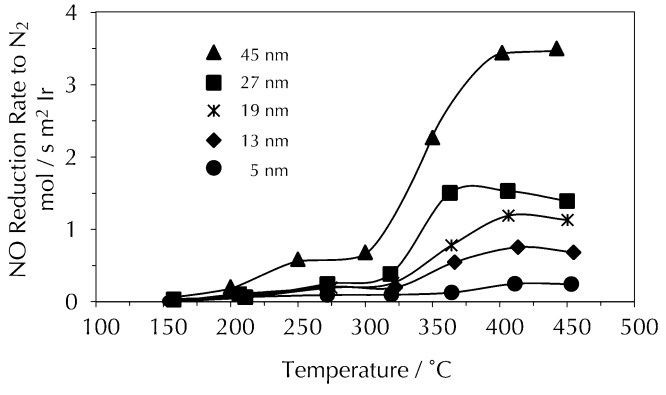

FIG. 6. Catalytic reduction of NO to N_2 vs temperature over Ir black expressed as reduction rate in moles NO converted to N_2 per second and square meter of the metal surface area. The crystallite sizes of the Ir black samples range from 5 to 45 nm. Data were obtained from mixtures of Ir black with SiO_2 after prereduction.

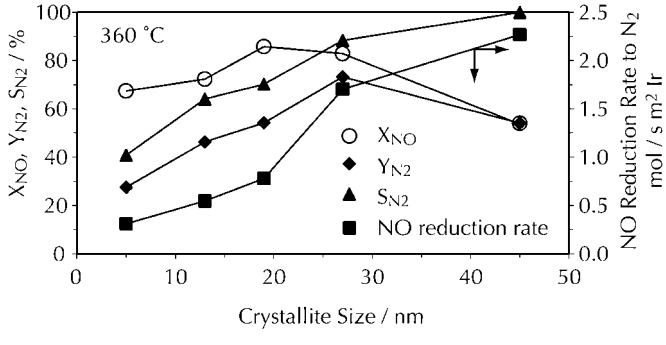

FIG. 7. The influence of Ir crystallite size on total NO conversion X_{NO}, NO conversion to N_2 (Y_{N_2}), selectivity to N_2 (S_{N_2}), and reduction rate expressed as moles NO converted to N_2 per second and square meter of the metal surface area at 360°C. Data were obtained from mixtures of Ir black with SiO_2 after prereduction. Note that rates correspond to different conversion levels due to the different activity at 360°C of the Ir black samples with different crystallites size.

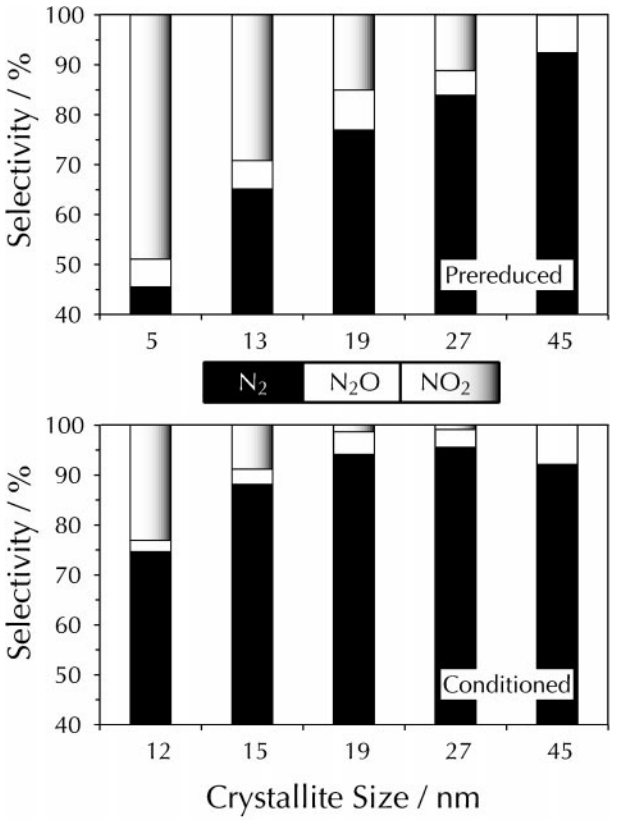

FIG. 8. Dependence of the selectivity to N_2, N_2O, and NO_2 on the Ir crystallite size and on pretreatment (prereduction or conditioning). The selectivities were calculated from the total amounts of products over the whole experimental temperature range from 160 to 460°C.

two different crystallite sizes contribute to the broadening of the main reflection (101) of IrO_2. The IrO_2-A with the smallest crystallites was the most susceptible material to the conditioning treatment. In comparison, the much better crystalline IrO_2-B showed low Y_{N_2} after calcination at 450°C in air, which increased only slightly after conditioning (Fig. 11). After *in situ* reduction of IrO_2-B at 300°C with 6% H_2 the activity increased tremendously, comparable to the activity of samples of Ir black with similar crystallite size. The reduction of IrO_2-B led to Ir with a crystallite size of 11 nm, after conditioning the crystallite size of Ir increased to 17 nm. This clearly indicates that IrO_2 cannot be the active phase in the reduction of NO by propene but it is important to note that though Ir^o produced by reduction of IrO_2-B exhibited high activity, conditioning further increased Y_{N_2}. From the morphological point of view IrO_2-A and IrO_2-B are distinct in many respects. Figure 12 compares the morphology of IrO_2-B with 24 nm and IrO_2-A with 17 nm crystallite size. IrO_2-B is made up of long needle-like particles of more than 100 nm in size and lumps of IrO_2, whereas no needles can be seen in the sintered form of IrO_2-A and only small, geometrically formed particles can be found. These differences in shape, crystallite size, and particle size are also reflected in the reduction behaviour of both IrO_2 samples as will be discussed below.

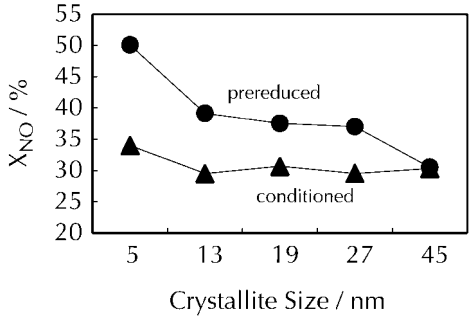

FIG. 9. Dependence of total NO conversion over the whole temperature range from 160 to 460°C on Ir crystallite size and pretreatment.

TABLE 5

Sintering Temperature, Crystallite Size, Specific Surface Area, and Y_{N_2} at 410°C of Different Samples of IrO_2

IrO_2 sample	Calcination temperature [°C]	IrO_2 crystallite size [nm]	Surface area [m^2/g]	Y_{N_2} at 410°C [%]
IrO_2-A	—	5	29.2 ± 0.5	45
IrO_2-A	750	17	13.9 ± 0.2	30
IrO_2-B	450	24	4.7 ± 0.1	<3

3.5. Reduction of NO_2 and N_2O with Propene

The only by-products in the selective catalytic reduction of NO with propene over unsupported Ir black were NO_2 and N_2O. NO_2 production exceeded N_2O production by far. To find evidence whether these two compounds are intermediates in the reduction of NO or whether they are simple by-products, a closer look was taken at the reduction of NO_2 and N_2O with propene under lean conditions and at the oxidation of NO to NO_2.

The results of the investigation of the catalytic activity of Ir black for NO oxidation to NO_2 are presented in Fig. 13a. The catalytic oxidation of ca. 300 ppm NO by 8% O_2 to NO_2 was carried out in a temperature-programmed experiment using a heating rate of 5 K/min. A maximum of approximately 70% of NO was oxidized to NO_2 between 310 and 330°C. Above this temperature the production of NO_2 is decreasing again due to the competing reaction of NO_2 decomposition at elevated temperatures as shown in Fig. 13b which depicts the decomposition of NO_2 in the presence of 1200 ppm O_2. In an atmosphere containing 8% O_2, decomposition of NO_2 was slowed down and shifted to higher temperatures. Above 300°C it followed the pattern of the oxidation of NO.

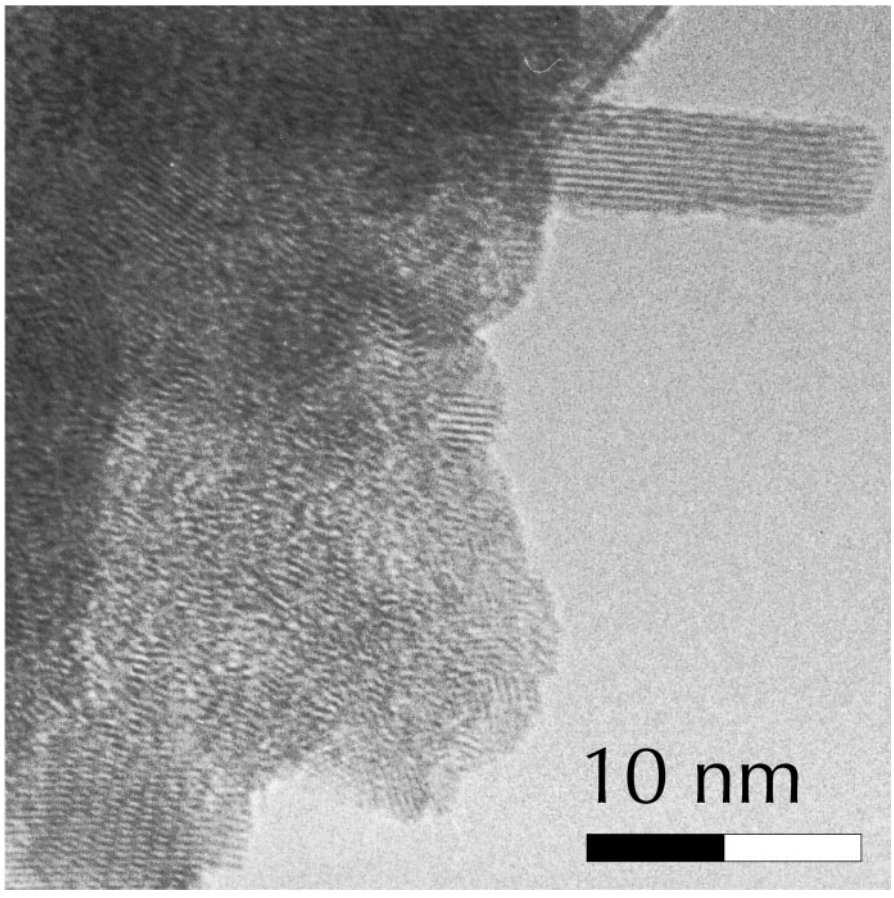

FIG. 10. TEM of IrO_2-A as received showing that the bulk material consists of crystallites in the range of 5 nm and some large crystallites (>10 nm). The dark and the white scaling bars are 5 nm in length.

To clarify the ability of propene to reduce NO_2 under oxidizing conditions, NO_2 was used as NO_x component. Figure 13c shows that in terms of Y_{N_2} no significant differences to experiments using NO arose (Y_{N_2} of an equivalent experiment using NO is included as dashed line). The reduction of NO_2 to NO is already observable at the starting temperature of the experiment (160°C) and is complete at 260°C. At 310°C reduction to N_2 sets in and follows the same pattern as the reduction of NO to N_2.

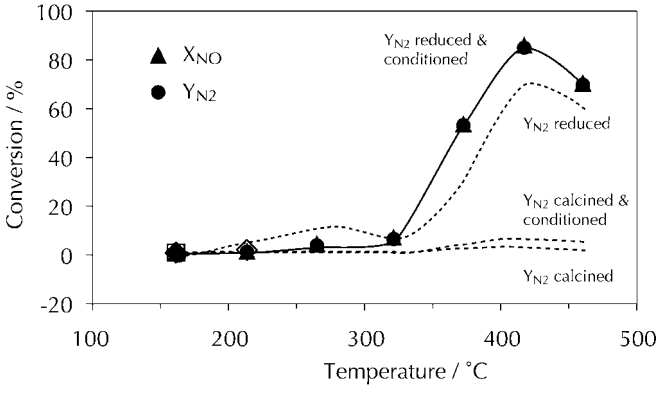

FIG. 11. Conversion of NO to N_2 (Y_{N_2}) and total NO conversion (X_{NO}) of IrO_2-B mixed with SiO_2 after reduction at 300°C with 6% H_2 and subsequent conditioning under reaction conditions at 450°C. For comparison Y_{N_2} for IrO_2-B mixed with SiO_2 after calcination at 450°C in air, calcined and conditioned, and directly after reduction are included as dashed lines.

Production of N_2O to a considerable degree was generally only observed with freshly reduced catalysts. Catalysts after reaction (conditioned catalysts) or when starting from IrO_2 usually were almost inactive for the reduction of NO to N_2O. This indicates that only metallic Ir is able to produce N_2O. In both steady-state and temperature-programmed experiments using N_2O as NO_x component, N_2O was not reduced by propene over Ir black under excess O_2; therefore the results are not shown here.

3.6. Redox Behaviour of Unsupported Iridium and IrO_2

The differences in crystallite size and sample morphology had a significant impact on the redox behaviour of the Ir and IrO_2 samples. This was checked for the oxidation and reduction behaviour of Ir with three different crystallite sizes (5, 13, 45 nm) and the three samples of IrO_2 used in this study (Table 5). The oxidation behaviour of Ir black

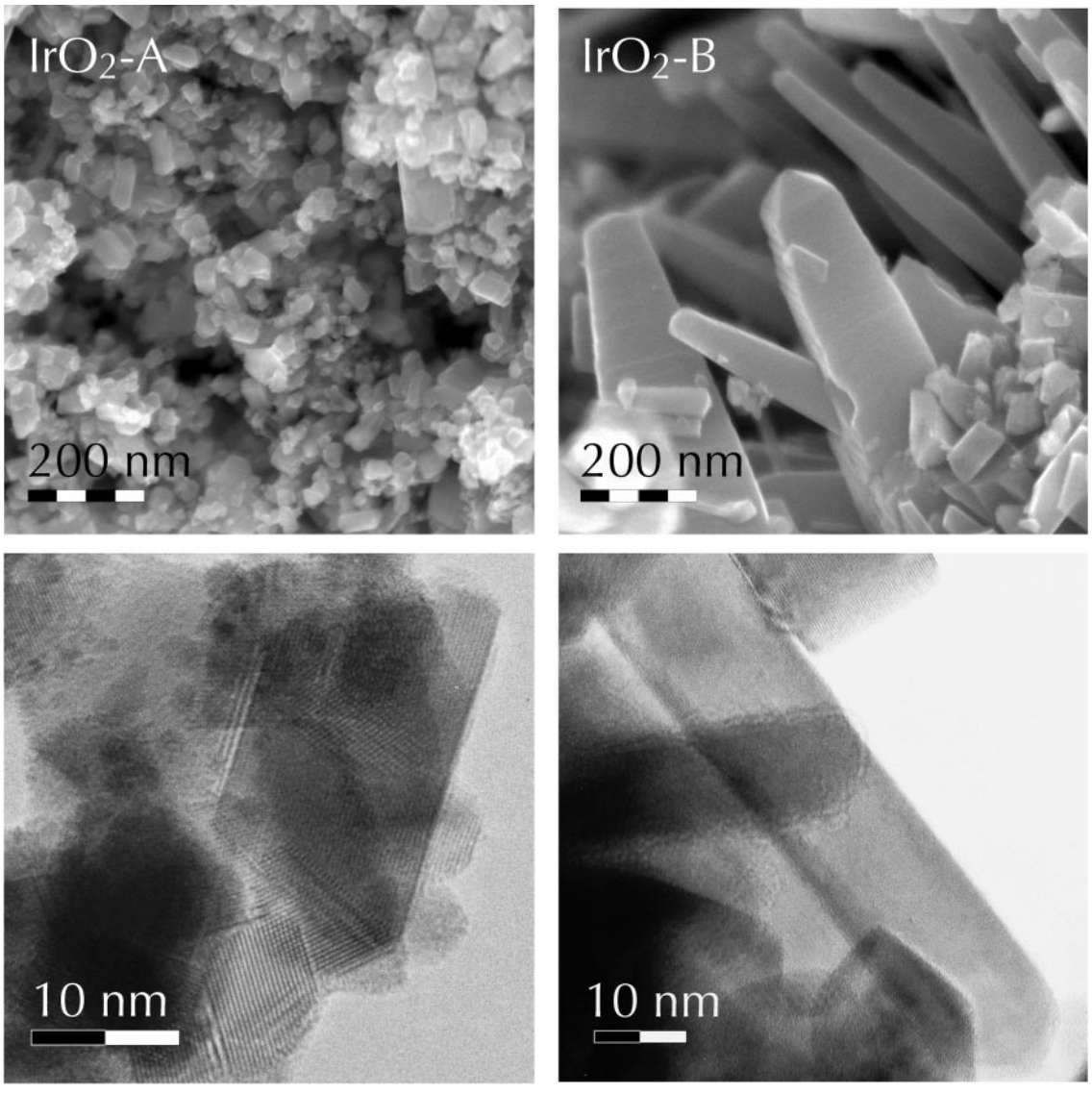

FIG. 12. Differences in morphology of IrO_2-A calcined at 750°C and IrO_2-B calcined at 450°C as evidenced by SEM (above) and TEM (below). The dark and white scaling bars are 50 and 5 nm in SEM and TEM micrographs, respectively.

with 5, 13, and 45 nm is compared in Fig. 14. The oxidation was performed with 20% O_2 in He with a heating rate of 5 K/min. It can be easily seen that Ir with the smallest crystallite size is oxidized most easily. Ir with the largest crystallite size cannot be fully oxidized under the applied conditions up to ca. 970°C, where the newly formed IrO_2 starts to be decomposed to metallic Ir and oxygen. At the maximum temperature of the catalytic tests (460°C) almost no oxidation takes place for the most sintered Ir sample. This is in accordance with the findings above, where Ir with 45 nm crystallite size is almost unchanged in activity and selectivity after conditioning at 450°C, whereas all the other samples change in activity, selectivity, and their degree of oxidation during time on stream.

The big differences in reduction behaviour of IrO_2-A as received, IrO_2-A calcined at 750°C, and IrO_2-B can shed some light on the different way these samples change during the conditioning procedure and on their different activity in NO reduction. With IrO_2-A as received reduction with H_2 proceeds in two distinct stages (Fig. 15). The first starts at temperatures below 100°C and is complete at approximately 150°C. The second becomes prominent just above 200°C and coincides with the reduction profiles of the other two samples. This again supports the previous observations by TEM and XRD that in IrO_2-A as received at least two morphologically different particles of IrO_2 are present. The reduction is complete at about 300°C in all three cases. The sintered sample of IrO_2-A and IrO_2-B are very similar in

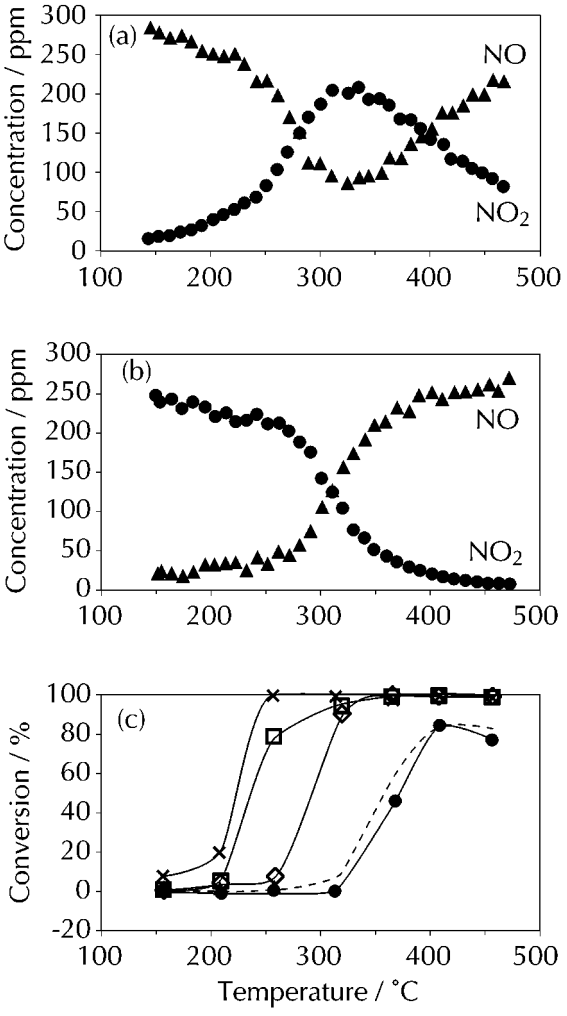

FIG. 13. Oxidation of ca. 300 ppm NO with 8% O_2 over Ir back mixed with SiO_2 (a). Decomposition of ca. 260 ppm NO_2 in the presence of ca. 1200 ppm O_2 (b). The heating rate was 5 K/min for (a) and (b). Catalytic behaviour of Ir black mixed with SiO_2 with NO_2 (300 ppm) as NO_x component in a steady-state measurement (c). Y_{N_2} of the experiment using NO as NO_x component is included for comparison and is presented as dashed line. ●, Y_{N_2}; ×, X_{NO_2}; ◇, $X_{Propene}$; □, X_{CO}.

reduction behaviour which is in accordance with their similar catalytic performance.

Oxidation and reduction experiments prove that in the investigated temperature range of the catalytic tests, IrO_2 can be easily reduced and Ir can be partly oxidized and that the redox behaviour is strongly dependent on crystallite size and the particle morphology.

4. DISCUSSION

The experiments using mechanical mixtures of Ir metal with various mixing materials conclusively prove that the support in the case of Ir is of minor importance to achieve high Y_{N_2} using propene as the main reducing agent and that

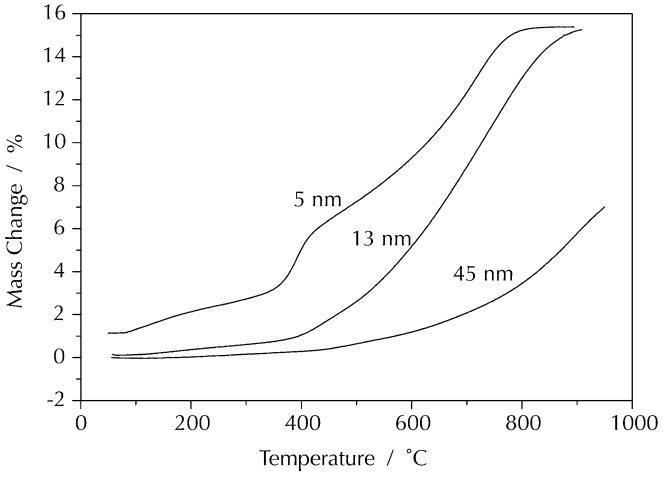

FIG. 14. Change of the mass as a function of temperature for Ir black samples with different crystallite sizes (5, 13, 45 nm) in 20% O_2 in He with a heating rate of 5 K/min.

Ir crystallite size has a strong impact on the performance of the catalyst. In the case of supported Ir catalysts the supports can be detrimental in two respects: either by stabilizing a high Ir metal dispersion and therefore keeping Ir crystallite size small or by exhibiting activity for the unselective oxidation or transformation of the reducing agent

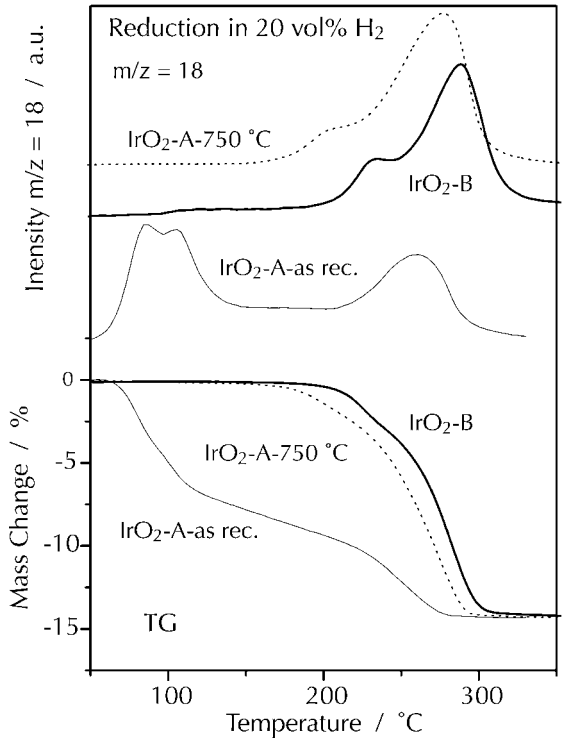

FIG. 15. Change of the mass (TG) and formation of water (mass spectrometric signal of $m/z = 18$) recorded during reduction of IrO_2-A as received, IrO_2-A calcined at 750°C, and IrO_2-B reduced by 20% H_2 in He with a heating rate of 10 K/min.

(11). Ir black is readily sintered and forms large aggregates with large crystallite size which show high selective conversions of NO to N_2.

The striking fact that selective reduction of NO to N_2 with propene using unsupported metallic iridium as a catalyst is favoured with increasing metal crystallite size, i.e., with decreasing surface area and dispersion, cannot be easily explained, and is unique among platinum group metals as shown above. For supported Ir catalysts it has already been shown that larger crystallite size favours the selective reduction of NO and that the catalyst in its most active state contains both phases, Ir and IrO_2 (12). Agglomeration and sintering of the metal seem to lower the influence of the support and thus enable Ir to exert its intrinsic catalytic activity. In fact, in the case of the most active samples of Ir-H-ZSM-5, we could confirm the presence of Ir crystals separated from the support (more than 50 nm in size) by TEM measurements (12). We suspect that the high activity of the Ir catalysts described by Nakatsuji (11) could arise from the generation of unsupported Ir due to the specific preparation method and the very severe calcination and pretreatment conditions which were applied. The differences in activity of the catalysts presented there can then be explained by the different degree of metal-support interaction which, in some cases, could be strong enough to keep the metal from sintering and from leaving the support, and in some cases the support could catalyse side reactions lowering the overall performance for NO reduction.

Oxidizability and reducibility of the Ir-IrO_2 system under reaction conditions seem to be the key for explaining the crystallite size dependence of the selective reduction of NO. Well crystalline IrO_2 is virtually inactive for NO reduction, whereas metallic Ir exhibits high Y_{N_2} with its magnitude depending on the crystallite size. This seems to indicate that metallic Ir is a necessary prerequisite for high selective NO reduction though an active participation of IrO_2 cannot be excluded because catalysts starting from metallic Ir after conditioning usually contain substantial amounts of IrO_2 and show improved performance compared to the pure metal even if crystallite size stays unchanged. The assumption that metallic Ir is mainly responsible for high Y_{N_2} is supported by the fact that the catalyst with the lowest surface area (Ir black with 45 nm) showed the highest conversion rates per Ir surface area and was oxidized up to 460°C to the lowest degree compared to the other samples. The trends can be summarized as follows: The larger the crystallite size, the higher the selectivity to N_2, and the lower the selectivity to NO_2 and the ability of Ir to be oxidized.

A better understanding of the mechanism of NO reduction with propene over PGMs would facilitate an explanation of the crystallite size dependence. Unfortunately, despite the plethora of mechanistic studies of this reaction on PGMs, no work on the mechanism using Ir as catalyst is available, and no general consensus has been reached so far for the other PGMs. In principle three general possible pathways can be distinguished and are most frequently invoked in the literature on PGMs, especially platinum (18):

(i) Direct NO decomposition on the metal and subsequent removal of oxygen by the hydrocarbon and thereby regenerating the active site (19, 20); a modification of this mechanism is the adsorbate-assisted NO decomposition, i.e., decomposition of NO assisted by fragments of propene (C_{ads}, C_xH_y, H_{ads}, etc.), as described by Burch and Watling (21);

(ii) Reduction of NO by oxygen-activated hydrocarbons (5); and

(iii) Reduction of NO_2 by the hydrocarbon (22). The first step in this reaction mechanism is the oxidation of NO to NO_2 over the PGMs and the subsequent reduction of the latter.

Our study demonstrates that Ir exhibits high activity for NO oxidation to NO_2. This constitutes a supporting fact for mechanism (iii). However, experiments using NO_2 as NO_x component showed that at lower temperatures Ir first reduces NO_2 to NO, whereas at higher temperatures the reduction proceeds to N_2 following the same pattern as with NO as NO_x component in the feed gas. This observation suggests that NO_2 is probably not a reaction intermediate, which is in line with the findings of Pitchon and Fritz (23), who proved in similar experiments with Pt catalysts that NO_2 is no reaction intermediate in HC-SCR. Furthermore, in the literature it is proposed that NO_2 could spill over to the support where it should be reduced by hydrocarbon-derived species (24). This should not be the case in our experiments due to the fact that Ir and support are physically separated in a mechanical mixture. Though our experiments indicate that NO oxidation is unlikely to be the first step in the DeNOx process using propene over Ir, the above results are not a sufficient proof justifying the exclusion of NO_2 as active species. NO_2 can still take part in the reaction as adsorbed reaction intermediate but we consider this as rather unlikely.

Mechanism (ii) requires the formation of an oxygen-containing hydrocarbon as reactive intermediate for the reduction of NO. Organic compounds containing carbonyl groups are well known to result from the partial oxidation of propene over Ir which proceeds via double bond cleavage of propene (25). Therefore the presence of activated hydrocarbons which are active as NO reductants is very likely, yielding mechanism (ii) as a feasible way for NO reduction.

An argument supporting mechanism (i) is the fact that NO decomposition over Ir is even more favoured than over Pt (26). A further supporting fact is the ability of propene to reduce IrO_2 under reaction conditions as shown in our

results: after conditioning metallic Ir was found in samples starting from IrO_2. On the other hand, hydrogen is a very effective reducing agent for the reduction of IrO_2 but it was shown by Burch and Coleman (27) that it is a poor reducing agent for NO reduction in excess oxygen over Ir. The same holds true for other reducing agents which, despite having a similar reducing power as propene for IrO_2 reduction, do not show any significant selective reduction of NO to N_2 in excess oxygen. These facts suggest an active role of the reductant in the reduction of NO beyond its ability of site regeneration by IrO_2 reduction. Preliminary results show that possibly decomposition products of propene assist in the removal NO. This will be the topic of a more detailed study.

A further important feature of unsupported Ir is that freshly reduced catalysts show relatively high selectivities for the production of N_2O (250 to 300°C) and that after conditioning, which leads to partial oxidation of the catalyst, this selectivity usually is reduced. This is very likely due to the fact that at those temperatures, where the production of N_2O sets in, O_2 is not able to already fully oxidize the Ir surface and thus the NO and N surface concentrations as well as NO mobility on the surface should be rather high, leading to the recombination of NO and N to N_2O. At least at these temperatures (250 to 300°C) on prereduced catalysts and under the applied conditions it is very likely that NO reduction proceeds via NO decomposition leading to N_2O and N_2.

Our results indicate that the most probable reaction pathway proceeds via the decomposition of NO over metallic Ir and subsequent removal of oxygen by the hydrocarbon. Especially for Ir with large crystallites this reaction pathway is very likely due to the fact that large Ir crystals are not easily oxidized but reduction of IrO_2 can proceed readily under the applied reaction conditions. Therefore, in this case the concentration of surface oxygen should be low. We cannot exclude that on Ir catalysts with small crystallite size and catalysts which are oxidized to a substantial degree after conditioning, NO reduction could proceed via a different mechanism. Due to the fact that it is very likely that the surface of Ir catalysts with small Ir crystallite size is fully oxidized, NO reduction could proceed via the formation of an oxygen-activated hydrocarbon in a similar way as suggested for Pt catalysts by Pitchon and Fritz (23).

5. CONCLUSIONS

We have shown that unsupported Ir black is a highly active catalyst for the reduction of NO using propene as the main reducing agent in excess of oxygen. Ir black shows a strong crystallite size dependence for the selective reduction of NO to N_2, which is unique among the platinum metals. The lower oxidizability of Ir with large crystallite size seems to be the major factor leading to the observed high activity and selectivity. Though pure, well crystalline IrO_2 is not active in the reduction of NO to N_2 with propene, it seems that a certain degree of surface oxidation enhances the activity and selectivity to N_2. Therefore for high NO conversions to N_2 a certain optimal ratio of $Ir : IrO_2$ seems to be necessary and the establishment of this ratio is strongly dependent on the redox behaviour of the $Ir\text{-}IrO_2$ system which is largely determined by the iridium crystallite size. As established before for Pt, NO_2 and N_2O do not seem to be likely reaction intermediates during the reduction of NO with propene in excess oxygen.

ACKNOWLEDGMENTS

We thank dmc[2] Degussa Metals Catalyst Cerdec AG for financial support of this research project. Electron microscopy investigations carried out by Dr. M. Müller (SEM) and Dr. F. Krumeich (TEM) are gratefully acknowledged.

REFERENCES

1. König, A., Herding, G., Hupfeld, B., Richter, T., and Weidmann, K., *in* "Preprints, Fifth International Congress on Catalysis and Automotive Pollution Control, Brussels, Belgium" (N. Kruse, A. Frennet, and J.-M. Bastin, Eds.), Vol. 1, p. 17, 2000. To be published in Topics of Catalysis.
2. Tauster, S. J., and Murrell, L. L., *J. Catal.* **41**, 192 (1976).
3. Lester, G. R., Joy, G. C., and Brennan, J. F., *SAE* **780202** (1978).
4. Taylor, K. C., and Schlatter, J. C., *J. Catal.* **63**, 53 (1980).
5. Obuchi, A., Ohi, A., Nakamura, M., Ogata, A., Mizuno, K., and Ohuchi, H., *Appl. Catal. B* **2**, 71 (1993).
6. Bamwenda, G. R., Ogata, A., Obuchi, A., Oi, J., Mizuno, K., and Skrzypek, J., *Appl. Catal. B* **6**, 311 (1995).
7. Bourges, P., Lunati, S., and Mabilon, G., *Stud. Surf. Sci. Catal.* **116**, 213 (1998).
8. Takami, A., Takemoto, T., Iwakuni, H., Yamada, K., Shigetsu, M., and Komatsu, K., *Catal. Today* **35**, 75 (1997).
9. Hori, M., Okumura, A., Goto, H., and Horiuchi, M., *SAE* **972850**, 1 (1997).
10. Nakatsuji, T., Yasukawa, R., Tabata, K., Ueda, K., and Niwa, M., *Appl. Catal. B* **21**, 121 (1999).
11. Nakatsuji, T., *Appl. Catal. B* **25**, 163 (2000).
12. Wögerbauer, C., Maciejewski, M., Baiker, A., and Göbel, U., *in* "Preprints, Fifth International Congress on Catalysis and Automotive Pollution Control, Brussels, Belgium" (N. Kruse, A. Frennet, and J. M. Bastin, Eds.), Vol. 1, p. 203, 2000. To be published in Topics of Catalysis.
13. Nawdali, M., Praliaud, H., and Primet, M., *in* "Preprints, Fifth International Congress on Catalysis and Automotive Pollution Control, Brussels, Belgium" (N. Kruse, A. Frennet, and J.-M. Bastin, Eds.), Vol. 2, p. 107, 2000. To be published in Topics of Catalysis.
14. Wögerbauer, C., Maciejewski, M., Schubert, M. M., and Baiker, A., *Catal. Lett.*, in press.
15. Radtke, F., Köppel, R., and Baiker, A., *Catal. Today* **26**, 159 (1995).
16. Maciejewski, M., Müller, C. A., Tschan, R., Emmerich, W. D., and Baiker, A., *Thermochim. Acta* **295**, 167 (1997).
17. Bergeret, G., and Gallezot, P., *in* "Handbook of Heterogeneous Catalysis" (G. Ertl, H. Knözinger, and J. Weitkamp, Eds.), Vol. 2, p. 439. VCH: Weinheim, 1997.

18. Burch, R., and Millington, P. J., *Catal. Today* **26**, 185 (1995).
19. Burch, R., Millington, P. J., and Walker, A. P., *Appl. Catal. B* **4**, 65 (1994).
20. Burch, R., and Watling, T. C., *Catal. Lett.* **43**, 19 (1997).
21. Burch, R., and Watling, T. C., *Catal. Lett.* **37**, 51 (1996).
22. Tanaka, T., Okuhara, T., and Misono, M., *Appl. Catal.* **4**, L1 (1994).
23. Pitchon, V., and Fritz, A., *J. Catal*. **186**, 64 (1999).
24. Burch, R., and Watling, T. C., *Stud. Surf. Sci. Catal*. **116**, 199 (1998).
25. Cant, N. W., and Hall, W. K., *J. Catal*. **27**, 70 (1972).
26. Savkin, V. V., and Kislyuk, M. U., *Kinet. Catal. USSR* **37**, 555 (1996).
27. Burch, R., and Coleman, M. D., *Appl. Catal. B* **23**, 115 (1999).